

Shock Electrodeposition in Charged Porous Media

Ji-Hyung Han¹ and Martin Z. Bazant^{1,2}*

Departments of Chemical Engineering¹ and Mathematics², Massachusetts Institute of Technology, Cambridge, MA 02139, USA * Email: bazant@mit.edu

ABSTRACT

It is shown that surface conduction in porous media can drastically alter the stability and morphology of electrodeposition at high rates, above the diffusion-limited current. Copper electrodeposits are visualized by scanning electron microscopy and energy dispersive spectroscopy in cellulose nitrate membranes, whose pores are coated with positive or negative charged polymers. Above the limiting current, surface conduction inhibits growth in the positive membrane and produces irregular dendrites, while it enhances growth and suppresses dendrites behind a deionization shock in the negative membrane. The discovery of uniform growth contradicts quasi-steady “leaky membrane” models, which are in the same universality class as unstable Laplacian growth, and indicates the importance of transient electro-diffusion or electro-osmotic dispersion. Shock electrodeposition could be exploited for high-rate recharging of metal batteries or manufacturing of metal matrix composite coatings.

Pattern formation by electrodeposition has fascinated physicists for over thirty years since Brady and Ball¹ first attributed the mechanism of copper dendritic growth to diffusion-limited aggregation². It was later discovered that morphology selection is also influenced by electromigration and convection in free solutions³⁻¹⁰. Here, we report some surprising effects of electromigration on dendritic growth in porous media.

Suppressing dendrites in porous separators is the critical challenge for high-energy-density batteries with Li^{11,12}, Zn¹³, Na, Cd or other metal anodes. Protruding dendrites can promote side reactions and cause capacity fade or catastrophic short circuits^{11,12}. A natural strategy to enhance cycle life is to mechanically block dendrites¹⁴, e.g. with stiff polymer separators¹⁵, but dendrites are difficult to suppress without increasing internal resistance, since ions must still pass freely. Another strategy to retard dendritic growth is to manipulate ionic fluxes near the metal surface¹⁶⁻¹⁹. High Li⁺ transference number to the surface can be achieved by utilizing silica nanoparticles with tethered ionic-liquid anions²⁰ and hydrophilic separators²¹ and designing proper electrolyte²² with large anion and low viscosity to reduce ion concentration gradients during polarization. Motivated by the hypothesis that dendritic growth is triggered by space charge formation^{23,24}, several studies have shown that supplying extra anions by charged nanoparticle dispersion²⁵ or solvent-in-salt electrolyte²⁶ can improve battery cycling, but the mechanism is controversial (see below).

In this Letter, we demonstrate by direct imaging that porous media with thin electric double layers (“leaky membranes”²⁷) can either stabilize or destabilize metal electrodeposition, depending on the pore surface charge. Our model system consists of a cellulose nitrate membrane (CN) with positive or negative polyelectrolyte coatings sandwiched between copper electrodes in copper sulfate solutions. As in straight nanopores²⁸, current-voltage relations (Fig.

1a and 1b) show common plateaus around the diffusion-limited current because surface conduction is negligible compared to bulk electro-diffusion. Upon strong salt depletion at higher voltages (Fig. 1c), however, the positive leaky membrane reduces the cation flux²⁸, while negative one exhibits over-limiting current by surface conduction^{7,27,28}, which forms a deionization shock²⁹⁻³¹ ahead of the growth. We shall see that these nonlinear phenomena can profoundly influence electrodeposition.

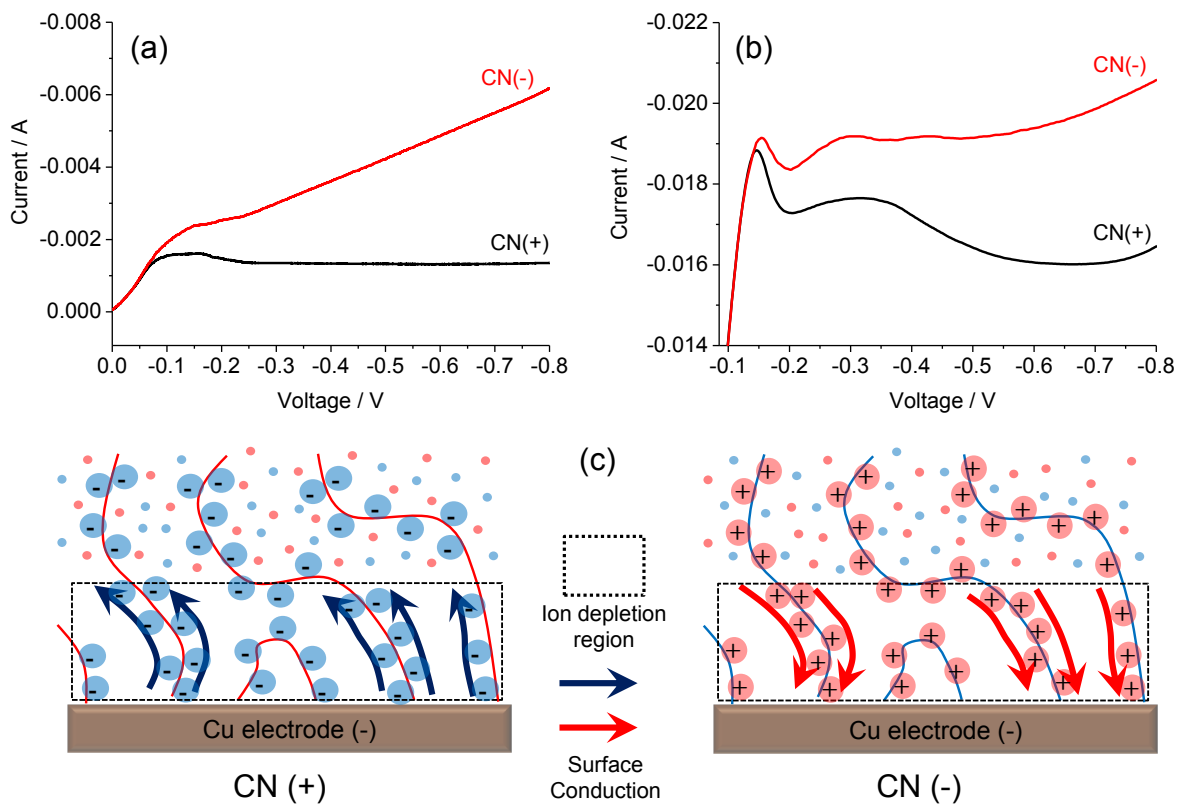


Fig. 1. Voltammetry of CN(+) and CN(-) membranes of exposed area 1.327 cm² between Cu electrodes in (a) 10 mM CuSO₄ at 1 mV/s and (b) 100 mM CuSO₄ at 10 mV/s. (c) Physical pictures of the effect of surface conduction on electrodeposition in a charged random porous media, driven by large electric fields in the ion depletion region.

Theory. – In free solutions, extended space charge is unlikely to form, according to theory³² and experiments on dendritic growth⁸ and electrodialysis^{30,33,34}. In the case of copper electrodeposition, morphological instability occurs upon depletion of the quasi-neutral electrolyte, which enhances ionic flux, avoids space charge, and preserves thin double layers^{7,16,35}. At the same time, the Rubinstein-Zaltzman hydrodynamic instability can lead to vortices that sustain over-limiting current (OLC), faster than electro-diffusion^{30,33,34,36,37}. This phenomenon is well established in electrodialysis^{30,33,34,37-40} and nanofluidics⁴¹ and may also explain electroconvection observed around dendrite tips^{3,8}.

In porous media, the physical mechanisms for OLC are very different and just beginning to be explored. According to theory⁷, supported by recent microfluidic experiments³¹, if the counterions (opposite to the pore surface charge) are being removed, then extended space charge is suppressed, and electro-osmotic instability is replaced by two new mechanisms for OLC: surface conduction by electromigration in submicron pores^{27,28}, and surface convection by electro-osmotic flow in micron-scale pores^{27,32,40,42}. If OLC is sustained at constant current^{29,43} or constant voltage⁴⁴, then the ion concentration profile develops an approximate discontinuity that propagates into the porous medium, leaving highly deionized fluid in its wake, until it relaxes to a steady linear profile in a finite porous slab^{27,45}. This “deionization shock wave” in the ion concentrations⁴³ is analogous to concentration shocks in chromatography, pressure shock waves in gases, stop-and-go traffic, glaciers, and other nonlinear kinematic waves⁴⁶.

The influence of surface conduction on electrodeposition was recently discovered, in the case of copper electrodeposits grown in the parallel nanopores of anodic aluminum oxide (AAO) membranes with modified surface charge²⁸. Below the limiting current, surface conduction is negligible if the double layers are thin (small Dukhin number), but surface conduction

profoundly affects the growth at high currents. With positive surface charge, growth is blocked at the limiting current by oppositely-directed surface conduction and convection; above a critical voltage, some dendrites are observed avoiding the pore walls, likely fed by vortices of reverse electro-osmotic flow returning along the pore centers. With negative surface charge, the growth is enhanced by surface conduction until the same critical voltage, when surface dendrites and ultimately smooth surface films grow rapidly along the walls. These phenomena are consistent with the theory of OLC in a single microchannel^{7,31}, but we expect different behavior in random media with interconnected porosity.

The theoretical motivation for our experiments is the prediction that a flat deionization shock is nonlinearly stable to shape perturbations⁴³, since this stability might be imparted to the electrodeposit growing behind the shock. In free solution, dendritic growth occurs soon after salt depletion, owing to the simple fact that a surface protrusion will receive more flux, thus causing it to protrude further¹, as shown in Fig. 2a. This is the fundamental instability mechanism of Laplacian growth, which leads to continuous viscous fingering⁴⁷ or fractal diffusion-limited aggregation (DLA)². In contrast, deionization shock propagation is controlled “from behind” by the high resistance of the ion depletion zone. As shown in Fig. 2b, a lagging region of the shock will have more flux leaving by surface conduction, causing it to advance back to the stable flat shape. The dynamics of a thin shock is equivalent to Laplacian dissolution⁴³, the stable time reversal of Laplacian growth⁴⁸.

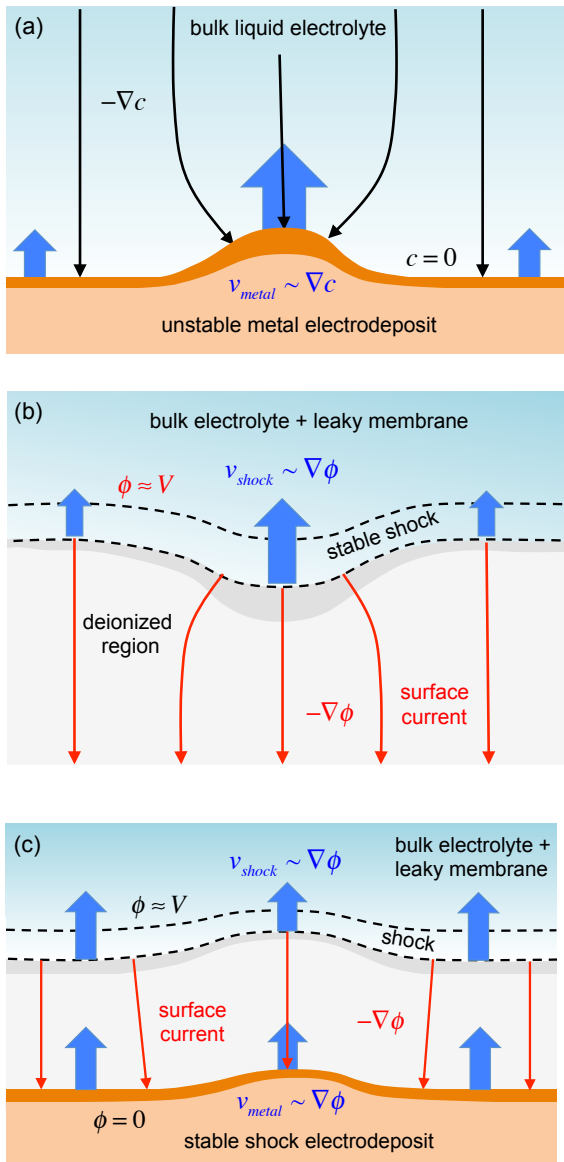


Fig. 2 Basic physics of shock electrodeposition. (a) Dendritic instability of electrodeposition in free solution. (b) Stability of deionization shock propagation in a leaky membrane. (c) Stabilization of electrodeposition behind a deionization shock.

What would happen if a stable deionization shock precedes an unstable growing electrodeposit in a charged porous medium? Using the “leaky membrane” model^{27,43,45} (LMM), which has various limitations (discussed below) but provides a convenient and well studied⁴⁹

mathematical framework, the answer depends on the importance of transient diffusion ahead of the shock. In the LMM, the ion concentrations $c_i(\vec{x}, t)$ and electrostatic potential of mean force $\phi(\vec{x}, t)$ satisfy the Nernst-Planck equations,

$$\frac{\partial c_i}{\partial t} + \vec{u} \cdot \nabla c_i = -\nabla \cdot \vec{F}_i = \nabla \cdot (D_i \nabla c_i + z_i e M_i c_i \nabla \phi) \quad (1)$$

coupled with macroscopic electroneutrality,

$$\sum_i z_i e c_i + \rho_s = 0 \quad (2)$$

including the surface charge density per volume, ρ_s , and the mean flow is incompressible and driven by gradients in dynamical pressure, electrostatic potential, and entropic chemical potential, respectively,

$$\nabla \cdot \vec{u} = 0, \quad \vec{u} = -k_D \nabla p - k_{EO} \nabla \phi - k_{DO} \nabla \ln c_i. \quad (3)$$

We assume that the macroscopic ionic diffusivities, D_i , and mobilities, M_i , Darcy permeability, k_D , electro-osmotic mobility, k_{EO} , and diffusio-osmotic mobility, k_{DO} , depend on c_i and ϕ , but not on their gradients or (explicitly) on position. This approximation is reasonable for surface conduction in nanopores, but neglects hydrodynamic dispersion, $D_i(\vec{u})$, due to electro-osmotic flow in micron-sized pores⁵⁰ or pore network loops⁴⁰, for which no simple model is available^{32,42}. For transport-limited electrodeposition, we further assume Dirchlet ($c_i = \phi = 0$) and Neumann ($\hat{n} \cdot \vec{u} = 0$) boundary conditions on the electrode surface.

With these broad assumptions, we observe that the steady-state LMM, Eqs. (1)-(3), is conformally invariant⁵¹. The profound implication is that *quasi-steady* transport-limited growth in a leaky membrane (with growth velocity opposite to the active-ion flux, $\vec{v} \sim -\vec{F}_1$) is in the same universality class⁵² as Laplacian growth^{53,54} and thus always unstable. This mathematical insight explains the recent theoretical prediction that negative charge in a leaky membrane

cannot stabilize quasi-steady electrodeposition, although it can reduce the growth rate of the instability⁵⁵, consistent with the improved cycle life of a lithium metal battery with “tethered anions” in the porous separator^{20,25}.

On the other hand, copper electrodeposition experiments in free solution have shown that the salt concentration profile is *unsteady* prior to interfacial instability³⁵ and forms a “diffusive wave” ahead of growing dendrites^{4,7} with the same asymptotic profile as a deionization shock⁴³. In a negatively charged porous medium, as the salt concentration vanishes at Sand’s time, the diffusion layer sharpens and propagates away from the electrode as deionization shock^{27,45}, which could perhaps lead to stable, uniform “shock electrodeposition” in its wake, as sketched in Fig. 2c. Since the LMM neglects many important processes, however, such as surface diffusion⁵⁶, surface convection^{32,50,56}, pore-scale heterogeneity⁵⁷, and electro-hydrodynamic dispersion^{40,42,50}, we turn to experiments to answer this theoretically motivated question.

Experiments. – In order to isolate effects of charged porous media, we use the same copper system (Cu|CuSO₄|Cu) studied by physicists for over three decades as the canonical example of diffusion-limited growth in free solutions^{1,3}. See Supporting Information for details. Compared to lithium electrodeposition, which involves complex side reactions and SEI formation, this system is simple enough to allow quantitative interpretation of voltammetry in nanopores²⁸ and microchannels^{3,7,35}. A unique feature of our experiments is that we control the surface conductivity, keeping all other conditions the same, by modifying the surface charge of the porous separator by layer-by-layer (LBL) deposition of charged polymers. We also demonstrate the role of *pore connectivity* for the first time by choosing a random porous material, cellulose nitrate (CN), with similar pore size (200~300 nm) as the parallel nanopores of AAO from our recent study that introduced this method²⁸. We denote the charge-modified positive and negative

membranes as CN(+) and CN(-), where excess sulfate ions (SO_4^{2-}) and cupric ions (Cu^{2+}), respectively, are the dominant counter-ions involved in surface conduction through the double layers (Fig. 1c).

As noted above, voltammetry clearly shows the nonlinear effect of surface conduction. Fig. 1a shows current-voltage curves of CN(+) and CN(-) in 10 mM CuSO_4 at a scan rate of 1 mV/s, close to steady state. In the low-voltage regime of slow electrochemical reactions²⁸ (below -0.07V), the two curves overlap since the double layers are thin, and surface conduction can be neglected compared to bulk diffusion (small Dukhin number)^{27,40}. At the diffusion-limited current, huge differences in CN(+) and CN(-) are suddenly observed. While the current in the CN(+) reaches -1.5 mA around -0.1 V and maintains a limiting current of -1.3 mA, the CN(-) shows a strong linear increase in current, i.e. constant over-limiting conductance. The data are consistent with the SC mechanism (Fig. 1c), which is sensitive to the sign of surface charge^{28,50}. With negative charge, Cu^{2+} counter-ions provide surface conduction to “short circuit” the depletion region to maintain electrodeposition. With positive charge, the SO_4^{2-} counter-ions migrate away from the cathode, further blocking Cu^{2+} ions outside the depletion region in order to maintain neutrality. At higher salt concentration, 100 mM CuSO_4 , sweeping at 10 mV/s, the results are similar (Fig. 1b) with no effect of SC below -0.15V, limiting current of -19 mA for CN(+), and overlimiting conductance for CN(-), although the effect of SC is weaker (smaller Dukhin number), and transient current overshoot and oscillations are observed^{28,58}.

The sensitivity of OLC electrodeposition to pore surface charge is truly striking. When constant OLC, -5 mA, is applied in 10 mM CuSO_4 solution (Fig. 3a), CN(+) shows unstable voltage variation, which we attribute to the complete blocking of cation transport in front of the cathode by the reverse SC of SO_4^{2-} counter-ions. This leads to large electric fields in the

depletion region that drive side reactions such as water electrolysis, consistent with observed gas bubbles. Moreover, electrodeposition is strongly suppressed from entering the CN(-) membrane, so it is easily separated from the cathode after the experiment. In stark contrast, CN(-) maintains low voltage around -100 mV, as expected since the SC of Cu^{2+} counter-ions sustains electrodeposition under OLC regime. More importantly, the electrodeposited Cu film in CN(-) is perfectly uniform (Fig. 3b), consistent with the theoretical motivation above, based on the stability of deionization shock propagation ahead of the growth. We are not aware of any previous observation of uniform metal growth in a porous medium, under the same conditions (dilute salt concentration and over-limiting current) where the growth would be unstable in free solution. We refer to this phenomenon as “shock electrodeposition”.

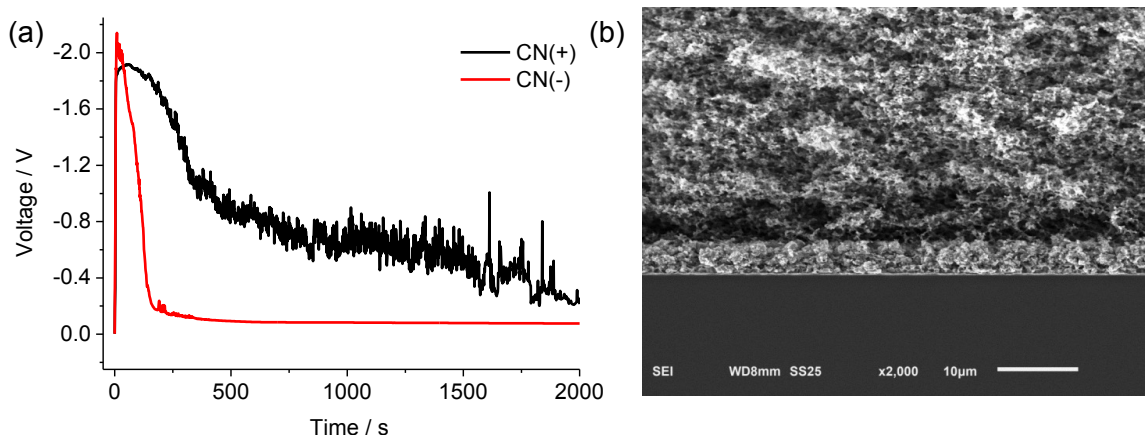


Fig. 3. (a) Chronopotentiometry data for CN(+) and CN(-) membranes at -5 mA for 2000 s in 10 mM CuSO_4 . (b) SEM image of a uniform Cu film in CN(-) grown by shock electrodeposition during OLC.

Figure 4 clearly shows the suppression of dendritic instability. When OLC (-20 mA) is applied in 100 mM CuSO_4 for 2000 s, irregular electrodeposits are generated in CN(+) (Fig. 4a).

This imposed current exceeds the limiting current (-17 mA) measured by voltammetry (Fig. 1b), so the observed low-density stochastic growth, which is opposed by surface conduction, may result from vortices of surface electroconvection, driven in the reverse direction by huge electric field in the depletion region. Once again, under the same experimental conditions, we obtain a highly uniform Cu film in CN(-) (Fig. 4b) by shock electrodeposition.

The difference in morphology of Cu electrodeposits between CN(+) and CN(-) can also be precisely confirmed by EDS mapping analysis of Cu element (Fig. 4c and 4d). The Cu film in CN(-) shows more compact and flat morphology, consistent with simple estimates of the metal density. Based on the applied current (20 mA), nominal electrode area (1.0 cm x 1.5 cm) and time (2000s), pure copper would reach a thickness of 19.6 μm , which would be increased by porosity, but also lowered by fringe currents, side reactions, and metal growth underneath the membrane. The much greater penetration of copper dendrites in CN(+) to a mean distance of 45 μm , supports the direct observation of low density ramified deposits. In contrast, the smaller observed penetration of 12.8 μm into CN(-) suggests that the shock electrodeposit densely fills the pores.

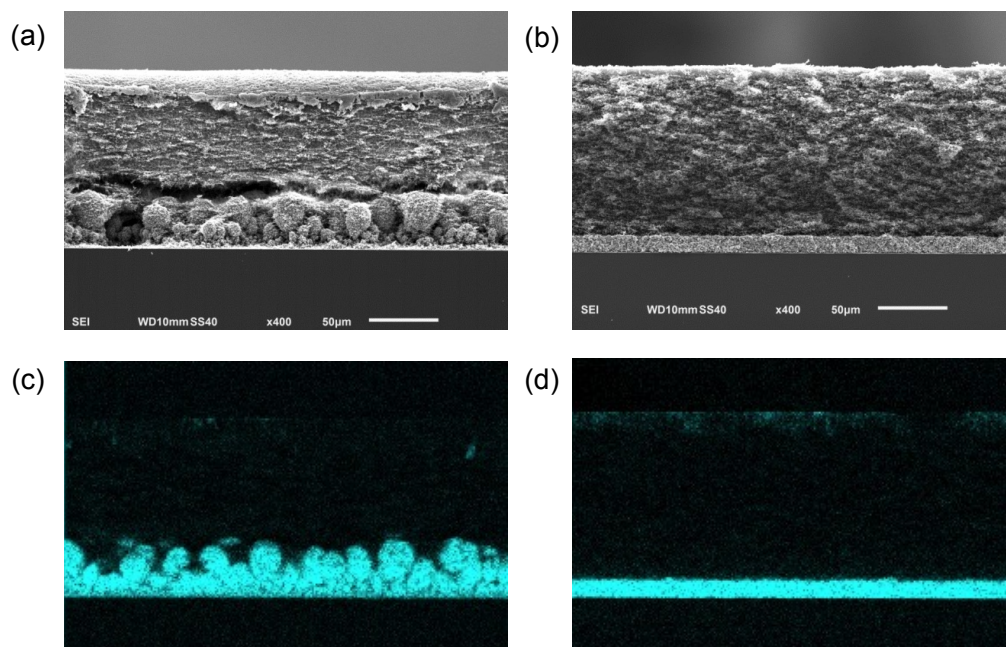


Fig. 4. Morphologies of Cu film depending on surface charge of CN membrane: CN(+) (a and c) and CN(-) (b and d). Cu electrodeposition is carried out in 100 mM CuSO₄ by applying -20 mA for 2000 s. SEM images (a and b) and EDS mapping analysis of Cu element (c and d).

The variation of morphology with applied current is demonstrated in Fig. 5. For under-limiting current (-15 mA), both cases exhibit a uniform Cu film (Fig. 5a and 5b), independent of surface charge, as expected when surface conduction is weak compared to bulk electro-diffusion within the pores (small Dukhin number). As the applied current is increased, highly irregular, dendritic electrodeposits are generated in CN(+). When extreme OLC (-25 mA) is applied, CN(+) shows much less dense dendritic growth, and weak adhesion of the membrane to the cathode leading to its peeling off (Fig. 5e). On the other hand, shock electrodeposition in CN(-) suppresses dendritic growth and produces uniform, dense Cu films, which show signs of instability only at very high currents (Fig. 5f).

The observed morphologies shed light on the different cycling behavior for positive and negative membranes under extreme currents (± 25 mA), as shown in Fig. 5g. The unstable dendritic growth of CN(+) results in short-circuit paths that cause the voltage to drop quickly to 5 mV in the first cycle. Although further cycles are possible, the voltage never recovers. In contrast, the more uniform growth observed in CN(-) is associated with stable cycling around ± 100 mV, in spite of the large nominal current density (± 18.8 mA/cm²), well above the limiting current. After eleven cycles the voltage drops to 30 mV, but further cycling is still possible without short circuits. Improved cycling life has also recently been reported for lithium metal anodes with separators having tethered anions⁵⁹, albeit at much lower currents (0.5 mA/cm²) without any observation of the deposits. Therefore, the phenomenon of stable shock electrodeposition, revealed by our imaging and analysis, may have broad applicability, including rechargeable metal batteries.

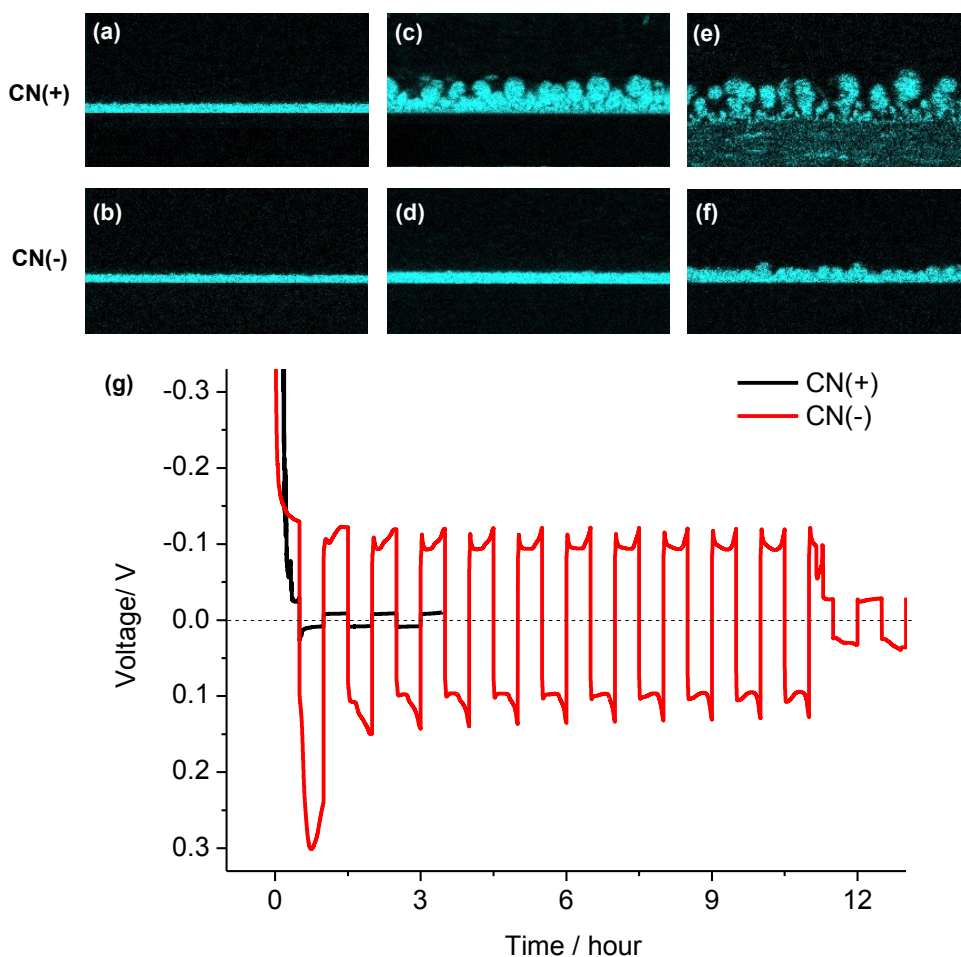


Fig. 5. EDS mapping analysis of Cu element. Cu is electrodeposited in CN(+) (a, c, e) and CN(-) (b, d, f) membranes at constant current densities in 100 mM CuSO_4 for 2000s (a, b) -15 mA, (c, d) -20 mA, and (e, f) -25 mA. (g) Galvanostatic cycling profiles of CN(+) and CN(-) using a symmetric copper cell: Cu is electrodeposited and electrodisolved under extreme OLC (25 mA) for 1800 s in 100 mM CuSO_4 .

Conclusion. – This work provides fresh insights into the physics of pattern formation. We show that surface conduction in a random porous medium can strongly influence the morphology of copper electrodeposition, which has been studied for decades in physics as the prototypical

case of unstable diffusion-limited growth. For the first time, we visually demonstrate the suppression of dendritic instability at high rates, exceeding diffusion limitation. With negative surface charge, uniform metal growth is stabilized behind a propagating deionization shock, and reversible cycling is possible. Under the same conditions with positive surface charge, the growth is highly unstable and cannot be cycled.

Besides its fundamental interest, shock electrodeposition may also find important engineering applications. As noted above, high-rate rechargeable metal batteries could be enabled by charged porous separators or charged composite metal electrodes^{11-13,60}. The rapid growth of dense, uniform metal electrodeposits in charged porous media could also be applied to the manufacturing of copper⁶¹ or nickel¹⁰ metal matrix composites for abrasives or wear-resistant coatings.

This work was supported by Saint Gobain Ceramics and Plastics, Northboro Research and Development Center and by Robert Bosch LLC through the MIT Energy Initiative. J.-H. H. also acknowledges initial support from the Basic Science Research Program of the National Research Foundation of Korea funded by the Ministry of Education (2012R1A6A3A03039224).

References

1. Brady, R. M. & Ball, R. C., Fractal growth of copper electrodeposits. *Nature* **309**, 225-229 (1984)
2. Witten, T. A. & Sander, L. M., Diffusion-limited aggregation, a kinetic critical phenomenon. *Phys. Rev. Lett.* **47**, 1400-1403 (1981)
3. Rosso, M., Electrodeposition from a binary electrolyte: new developments and applications. *Electrochim. Acta* **53**, 250–256 (2007)
4. Fleury, V., Rosso, M., Chazalviel, J. N. & Sapoval, B., Experimental aspects of dense morphology in copper electrodeposition. *Phys. Rev. A* **44**, 6693-6705 (1991)

5. Barkey, D. & Laporte, P., The dynamic diffusion layer in branched growth of a conductive-polymer aggregate in a 2-D electrolysis cell. *J. Electrochem. Soc.* **137**, 1655-1656 (1990)
6. Bazant, M. Z., Regulation of ramified electrochemical growth by a diffusive wave. *Phys. Rev. E* **52**, 1903-1914 (1995)
7. Léger, C., Elezgaray, J. & Argoul, F., Dynamical characterization of one-dimensional stationary growth regimes in diffusion-limited electrodeposition processes. *J. Phys. Rev. E* **58**, 7700-7709 (1998)
8. Huth, J. M., Swinney, H. L., McCormick, W. D., Kuhn, A. & Argoul, F., Role of convection in thin-layer electrodeposition. *Phys. Rev. E* **51**, 3444-3458 (1995)
9. Erlebacher, J., Searson, P. C. & Sieradzki, K., Computer simulations of dense-branching patterns. *Phys. Rev. Lett.* **71**, 3311-3314 (1993)
10. Grier, D., Ben-Jacob, E., Clarke, R. & Sander, L. M., Morphology and microstructure in electrochemical deposition of zinc. *Phys. Rev. Lett.* **56**, 1264 (1986)
11. Xu, W. *et al.*, Lithium metal anodes for rechargeable batteries. *Energ. Environ. Sci.* **7**, 513-537 (2014)
12. Aurbach, D., Zinigrad, E., Cohen, Y. & Teller, H., A short review of failure mechanisms of lithium metal and lithiated graphite anodes in liquid electrolyte solutions. *Solid State Ionics* **148**, 405-416 (2002)
13. Lee, J.-S. *et al.*, Metal-air batteries with high energy density: Li-air versus Zn-air. *Adv. Energy Mater.* **1**, 34-50 (2011)
14. Monroe, C. & Newman, J., The impact of elastic deformation on deposition kinetics at lithium/polymer interfaces. *J. Electrochem. Soc.* **152**, A396-A404 (2005)
15. Hallinan, D. T., Mullin, S. A., Stone, G. M. & Balsara, N. P., Lithium metal stability in batteries with block copolymer electrolytes. *J. Electrochem. Soc.* **160**, A464-A470 (2013)
16. Akolkar, R., Mathematical model of the dendritic growth during lithium electrodeposition. *J. Power Sources* **232**, 23-28 (2013)
17. Nishikawa, K., Fukunaka, Y., Sakka, T., Ogata, Y. H. & Selman, J. R., Measurement of concentration profiles during electrodeposition of Li metal from LiPF₆-PC electrolyte solution: The role of SEI dynamics. *J. Electrochem. Soc.* **154**, A943-A948 (2007)
18. Nishikawa, K., Mori, T., Nishida, T., Fukunaka, Y. & Rosso, M., Li dendrite growth and Li⁺ ionic mass transfer phenomenon. *J. Electroanal. Chem.* **661**, 84-89 (2011)
19. Ding, F. *et al.*, Dendrite-free lithium deposition via self-healing electrostatic shield mechanism. *J. Am. Chem. Soc.* **135**, 4450-4456 (2013)

20. Schaefer, J. L., Yanga, D. A. & Archer, L. A., High lithium transference number electrolytes via creation of 3-dimensional, charged, nanoporous networks from dense functionalized nanoparticle composites. *Chem. Mater.* **25**, 834-839 (2013)
21. Ryou, M.-H. *et al.*, Excellent cycle life of lithium-metal anodes in lithium-ion batteries with mussel-inspired polydopamine-coated separators. *Adv. Energy Mater.* **2**, 645-650 (2012)
22. Park, M. S. *et al.*, A highly reversible lithium metal anode. *Sci. Rep.* **4**, 3815 (2014)
23. Brissot, C., Rosso, M., Chazalviel, J. N. & Lascaud, S., Dendritic growth mechanisms in lithium/polymer cells. *J. Power Sources* **81-82**, 925-929 (1999)
24. Chazalviel, J. N., Electrochemical aspects of the generation of ramified metallic electrodeposits. *Phys. Rev. A* **42**, 7355-7367 (1990)
25. Lu, Y., Das, S. K., Moganty, S. S. & Archer, L. A., Ionic liquid-nanoparticle hybrid electrolytes and their application in secondary lithium-metal batteries. *Adv. Mater.* **24**, 4430-4435 (2012)
26. Suo, L., Hu, Y.-S., Li, H., Armand, M. & Chen, L., A new class of solvent-in-salt electrolyte for high-energy rechargeable metallic lithium batteries. *Nat. Commun.* **4**, 1481 (2013)
27. Dydek, E. V. & Bazant, M. Z., Nonlinear dynamics of ion concentration polarization in porous media: The leaky membrane model. *AIChE Journal* **59**, 3539-3555 (2013)
28. Han, J.-H., Khoo, E., Bai, P. & Bazant, M. Z., Over-limiting current and control of dendritic growth by surface conduction in nanopores. *Sci. Rep.* **4**, 7056 (2014)
29. Mani, A., Zangle, T. & Santiago, J., On the propagation of concentration polarization from microchannel–nanochannel interfaces Part I: analytical model and characteristic analysis. *Langmuir* **25**, 3898-3908 (2009)
30. Yossifon, G. & Chang, H.-C., Selection of nonequilibrium overlimiting currents: universal depletion layer formation dynamics and vortex instability. *Phys. Rev. Lett.* **101**, 254501 (2008)
31. Nam, S. *et al.*, Experimental verification of overlimiting current by surface conduction and electro-osmotic flow in microchannels. *Phys. Rev. Lett.* **114**, 114501 (2015)
32. Rubinstein, I. & Zaltzman, B., Convective diffusive mixing in concentration polarization: from Taylor dispersion to surface convection. *J. Fluid Mech.* **728**, 239-278 (2013)
33. Rubinstein, S. M. *et al.*, Direct observation of a nonequilibrium electro-osmotic instability. *Phys. Rev. Lett.* **101**, 236101 (2008)
34. Nikonenko, V. *et al.*, Intensive current transfer in membrane systems: Modelling, mechanisms and application in electrodialysis. *Adv. Colloid Interface Sci.* **160**, 101-123 (2010)

35. Elezgaray, J., Léger, C. & Argoul, F., Linear stability analysis of unsteady galvanostatic electrodeposition in the two-dimensional diffusion-limited regime. *J. Electrochem. Soc.* **145**, 2016-2024 (1998)
36. Zaltzman, B. & Rubinstein, I., Electro-osmotic slip and electroconvective instability. *J. Fluid Mech.* **579**, 173-226 (2007)
37. Nikonenko, V. V. *et al.*, Desalination at overlimiting currents: State-of-the-art and perspectives. *Desalination* **342**, 85-106 (2014)
38. Krol, J. J., Wessling, M. & Strathmann, H., Chronopotentiometry and overlimiting ion transport through monopolar ion exchange membranes. *J. Membrane Sci.* **162**, 155-164 (1999)
39. Balster, J. *et al.*, Morphology and microtopology of cation-exchange polymers and the origin of the overlimiting current. *J. Phys. Chem. B* **111**, 2152-2165 (2007)
40. Deng, D. *et al.*, Overlimiting current and shock electro dialysis in porous media. *Langmuir* **29**, 16167-16177 (2013)
41. Liu, Y., Huber, D. E. & Dutton, R. W., Limiting and overlimiting conductance in field-effect gated nanopores. *Appl. Phys. Lett.* **96**, 253108 (2010)
42. Yaroshchuk, A., Zholkovskiy, E., Pogodin, S. & Baulin, V., Coupled concentration polarization and electroosmotic circulation near micro/nanointerfaces: Taylor-Aris model of hydrodynamic dispersion and limits of its applicability. *Langmuir* **27**, 11710-11721 (2011)
43. Mani, A. & Bazant, M. Z., Deionization shocks in microstructures. *Phys. Rev. E* **84**, 061504 (2011)
44. Zangle, T., Mani, A. & Santiago, J., On the propagation of concentration polarization from microchannel-nanochannel interfaces Part II: numerical and experimental study. *Langmuir* **25**, 3909-3916 (2009)
45. Yaroshchuk, A., Over-limiting currents and deionization "shocks" in current-induced polarization: Local-equilibrium analysis. *Adv. Colloid Interface Sci.* **183-184**, 68-81 (2012)
46. Whitham, G. B. *Linear and Nonlinear Waves*. 1 edition edn, (Wiley-Interscience, 1999).
47. Bensimon, D., Kadanoff, L. P., Liang, S., Shraiman, B. I. & Tang, C., Viscous flows in two dimensions. *Rev. Mod. Phys.* **58**, 977-999 (1986)
48. Bazant, M. Z., Interfacial dynamics in transport-limited dissolution. *Phys. Rev. E* **73**, 060601 (2006)
49. Spiegler, K. S., Polarization at ion exchange membrane-solution interfaces. *Desalination* **9**, 367-385 (1971)

50. Dydek, E. V. *et al.*, Overlimiting current in a microchannel. *Phys Rev Lett.* **107**, 118301 (2011)
51. Bazant, M. Z., Conformal mapping of some non-harmonic functions in transport theory. *Proc. Roy. Soc. Math. Phys. Eng. Sci.* **460**, 1433-1452 (2004)
52. Bazant, M. Z., Choi, J. & Davidovitch, B., Dynamics of conformal maps for a class of non-Laplacian growth phenomena. *Phys. Rev. Lett.* **91**, 045503 (2003)
53. Hastings, M. B. & Levitov, L. S., Laplacian growth as one-dimensional turbulence. *Phys. D* **116**, 244-252 (1998)
54. Barra, F., Davidovitch, B. & Procaccia, I., Iterated conformal dynamics and Laplacian growth. *Phys. Rev. E* **65**, 046144 (2002)
55. Tikekar, M. D., Archer, L. A. & Kocha, D. L., Stability analysis of electrodeposition across a structured electrolyte with immobilized anions. *J. Electrochem. Soc.* **161**, A847-A855 (2014)
56. Nielsen, C. P. & Bruus, H., Concentration polarization, surface currents, and bulk advection in a microchannel. *Phys. Rev. E* **90**, 043020 (2014)
57. Mirzadeh, M., Gibou, F. & Squires, T. M., Enhanced charging kinetics of porous electrodes: Surface conduction as a short-circuit mechanism. *Phys. Rev. Lett.* **113**, 097701 (2014)
58. Moya, A. A., Belashova, E. & Sibat, P., Numerical simulation of linear sweep and large amplitude ac voltammetries of ion-exchange membrane systems. *J. Membrane Sci.* **474**, 215-223 (2015)
59. Lu, Y., Tu, Z. & Archer, L. A., Stable lithium electrodeposition in liquid and nanoporous solid electrolytes. *Nat. Mater.* **13**, 961-969 (2014)
60. Ellis, B. L. & Nazar, L. F., Sodium and sodium-ion energy storage batteries. *Curr. Opin. Solid State Mater. Sci.* **16**, 168-177 (2012)
61. Zhu, J., Liu, L., Zhao, H., B., S. & Hu, W., Microstructure and performance of electroformed Cu/nano-SiC composite. *Mater. Des.* **28**, 1958-1962 (2007)

Shock Electrodeposition in Charged Porous Media

Supporting Information: Experimental Methods

*Ji-Hyung Han*¹ and *Martin Z. Bazant*^{1,2*}

Departments of Chemical Engineering¹ and Mathematics², Massachusetts Institute of Technology, Cambridge, MA 02139, USA * Email: bazant@mit.edu

Two copper (Cu) disk electrodes (diameter 13 mm, thickness 2 mm) are used as the working and counter electrodes. Electrode polishing consists of grinding by fine sand paper (1200, Norton) followed by 3.0 μm alumina slurry (No. 50361-05, Type DX, Electron Microscopy Sciences) and thorough rinsing with purified water. All chemicals including Polydiallyldimethylammonium chloride (pDADMAC, 100,000 ~ 200,000 M_w), (poly(styrenesulfonate) (PSS, 70000 M_w), copper sulfate (CuSO_4), sodium chloride (NaCl), and sodium hydroxide (NaOH) are purchased from Aldrich and used without further purification. Ultrapure deionized water is obtained from Thermo Scientific (Model No. 50129872 (3 UV)). Cellulose nitrate (CN) membranes (pore diameter 200~300 nm, porosity 0.66 – 0.88, thickness 130 μm , diameter 47 mm) are purchased from Whatman.

The surface charge of several CN membranes is modified by layer-by-layer (LBL) method of charged polyelectrolytes. Polydiallyldimethylammonium chloride (pDADMAC) is directly deposited on the membrane to make a positive surface charge, CN(+). For this, the bare CN is

immersed in polycation solution (1 mg/mL pDADMAC in 20 mM NaCl at pH 6) for 30 min. Then, the membrane is thoroughly rinsed with purified water by three times (10 min for each) to remove unattached polyelectrolyte. Negatively charged CN(-) is obtained by coating negative polyelectrolytes (poly(styrenesulfonate), PSS) on the pDADMAC-coated CN. In this step, the pDADMAC coated CN is immersed in polyanion solution (1 mg/mL PSS in 20 mM NaCl at pH 6) for 30 min and followed by the same cleaning procedure. The polyelectrolytes coated CN membranes are stored in CuSO₄ solution.

The experimental setup is from previous our work¹. The CN membrane is clamped between two Cu disk electrodes (diameter 13 mm) under constant pressure, where copper electrodeposits at the cathode and dissolves at the anode. For SEM images, Cu sputtered Si wafer (1.0 cm × 1.5 cm) is used as a cathode. In order to prevent the evaporation of the binary electrolyte solution inside the CN membrane, the electrochemical cell is immersed in a beaker containing the same electrolyte. All electrochemical measurements are performed with a potentiostat (Reference 3000, Gamry Instruments). The morphology and composition of electrodeposited Cu films are confirmed by scanning electron microscopy (SEM) with energy-dispersive (EDS) X-ray spectroscopy detector (6010LA, JEOL) at 15 kV accelerating voltage.

REFERENCE

1. Han, J.-H., Khoo, E., Bai, P. & Bazant, M. Z., Over-limiting current and control of dendritic growth by surface conduction in nanopores. *Sci. Rep.* **4**, 7056 (2014).